

Photorefractive recording in ac-biased cadmium telluride

K. Shcherbin^{a,*}, V. Danylyuk^a, Z. Zakharuk^b, I. Rarenko^b, M.B. Klein^c

^a Institute of Physics, Prospekt Nauki 46, Kiev 03650, Ukraine

^b Chernivtsy National University, Kotsyubinskogo Str. 2, Chernivtsy 58012, Ukraine

^c Lasson Technologies Inc., 6059 Bristol Parkway, Culver City, CA 90230, USA

Received 19 December 2002; received in revised form 30 January 2003; accepted 2 July 2003

Abstract

We report effect of external ac-field on photorefractive properties of CdTe:Ge at 1.06 μm . Phenomena related to excitation of the space-charge waves (SCW) of traps recharging, such as spatial subharmonics generation and resonant two-beam coupling, are studied. Dramatic enhancement of the photorefractive response is achieved in ac-biased crystal by adjustment of recording conditions (field and grating spacing) to eigen resonance related to excitation of the space charge waves.

© 2003 Elsevier B.V. All rights reserved.

PACS: 42.65.Hw; 42.70.Nq; 52.35.Mw; 72.80.Ey

Keywords: Semiconductors; Nonlinear optics

1. Introduction

Photorefractive effect is the light-induced change of refractive index in electro-optic materials when the space-charge field is formed under nonuniform illumination. High sensitivity of this phenomenon makes it attractive for many optical holographic processing applications. Traditional photorefractive materials are ferroelectric oxides like BaTiO₃ and LiNbO₃. These crystals exhibit large electro-optic constants and therefore ensure high photorefractive nonlinearity. However, response of these materials is usually slow and therefore ferroelectrics exhibit relatively low sensitivity, defined as refractive index change per absorbed photon density. Photorefractive semiconductors like CdTe, InP and GaAs possess the shortest response time and the best photorefractive sensitivity as compare to other photorefractive materials. That is why they are promising for fast image processing, real-time interferometry, optical information processing, etc. An additional advantage of photorefractive semiconductors is sensitivity in the near infrared and as a result compatibility with low cost light sources and existing telecommunication components pos-

sessing smallest dispersion and minimum losses just in this region of spectrum.

CdTe exhibits the largest electro-optic constant [1] among all known semiconductors and therefore has a grate potential for practical applications. Several dopants are known at present that form in cadmium telluride impurity levels involved in photoinduced charge redistribution and enhance in such a way photorefractive sensitivity. These are vanadium [2], vanadium co-doped with manganese [3], germanium [4] and tin [5]. It was shown that some germanium-doped samples ensure the largest photorefractive coupling strength among all semiconductors without applied electric field [6].

Being the largest among all semiconductors electro-optic constant of CdTe is still not sufficiently high for many applications. The photorefractive response can be improved by the external electric field. Two techniques are used now: in the first one a moving grating is recorded in the crystal with the applied dc field [7]; in the second approach the ac field is applied when a stationary grating is recorded [8]. Symmetric square-shaped ac field ensures larger optical nonlinearity. It was shown to be effective with CdTe [9]. In present work, we report enhancement of photorefractive response in germanium doped cadmium telluride achieved at 1.06 μm by means of square-shaped ac field.

* Corresponding author. Tel.: +380-44-265-0818; fax: +380-44-265-2359.

E-mail address: kshcherb@iop.kiev.ua (K. Shcherbin).

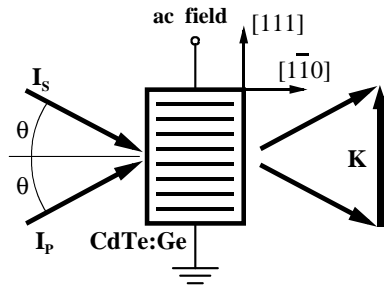


Fig. 1. Schematic sketch of the two-beam coupling experiment in CdTe.

2. Experimental set-up

CdTe:Ge crystal was grown by Bridgman technique in Chernovtsy National University, Ukraine. It is deliberately germanium-doped and exhibits dark conductivity of order of $10^{-9} \Omega \text{ cm}^{-1}$. Single crystal sample studied with dimensions $4 \text{ mm} \times 5 \text{ mm} \times 10 \text{ mm}$ was cut from the ingot along $[1\bar{1}\bar{2}]$, $[1\bar{1}1]$ and $[1\bar{1}0]$ directions, respectively. The input and output faces parallel to $(1\bar{1}1)$ crystallographic plane are optically finished while the side faces parallel to (111) plane are painted with silver paste. Nearly square-shaped ac voltage with frequency 700 Hz is applied to these faces.

Schematic sketch of optical waves intersection in the sample is shown in Fig. 1. The output beam of a single-mode single-frequency diode-pumped Nd^{3+} :YAG laser operating at $\lambda = 1.06 \mu\text{m}$ is split into two recording beams I_s and I_p with total intensity about 24 mW/cm^2 and intensity ratio $\beta \approx 1:1000$. These beams impinge upon the sample at an angle $2\theta \approx 1.4^\circ$ and form inside the crystal interference pattern with fringe spacing $\Lambda \approx 42 \mu\text{m}$. The interference fringes create periodically modulated space-charge field; the field results in refractive index change through the linear electro-optic effect. The recording beams are polarized in the plane of incidence, so the grating vector and the light polarization vectors are kept nearly parallel to $[1\bar{1}1]$ direction.

Photorefractive grating recorded in the presence of ac field is $\pi/2$ -shifted with respect to the interference pattern [8]. This asymmetry leads to directional energy transfer between two coupling beams: one beam is amplified at the expense of the other beam. We study temporal variation and steady state amplification of the weak signal beam I_s/I_{s0} , where I_s and I_{s0} are intensities of the weak signal beam in the presence and without pump beam, respectively. Also, in some experiments, a screen is placed behind the crystal and intensity pattern behind the sample is recorded by a CCD camera.

3. Experimental results and discussion

Temporal dynamics of the signal after switching on the pump beam are shown in Fig. 2 for different amplitudes of the applied field. For relatively low field, steady state signal amplification increases with field, as it is expected, and

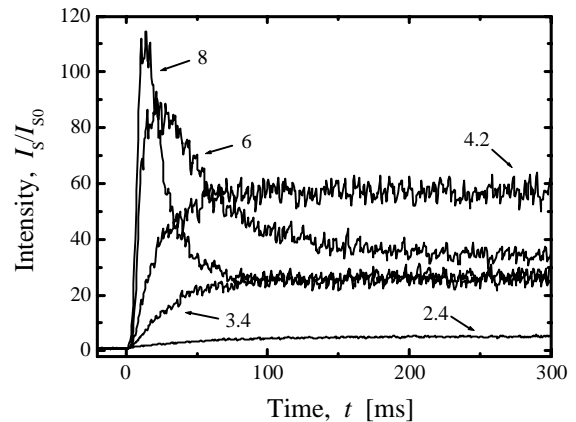


Fig. 2. Dynamics of the signal beam amplification for different amplitudes of the applied field; pump beam is switched on at $t = 0$; labels indicate external ac field in kV/cm.

nearly 60 times signal gain is reached at $E \approx 4.2 \text{ kV/cm}$. Typical smooth growth of the signal is observed until steady state value is reached. However, with further field increase temporal behavior of the signal changes dramatically: transient peak is observed after which signal decreases and steady-state gain becomes smaller even than at lower field. The steady state and maximum gain are plotted in Fig. 3 as a function of the field. While transient gain increases with field and reaches nearly 120 times at $E = 8 \text{ kV/cm}$ the steady state amplification decreases for $E > 4.4 \text{ kV/cm}$. Such behavior can not be explained within traditional photorefractive model [8], which predicts growth of the gain until traps saturation is reached.

To make clear the origin of unusual behavior of amplified beam we study intensity distribution behind the crystal. Pictures taken from screen placed at a distance of 1 m behind the sample are presented in Fig. 4. Upper picture shows transmitted beams when no field is applied. Middle picture corresponds to $E = 4.2 \text{ kV/cm}$; large signal beam amplification is obvious. Bottom picture shows intensity distribution

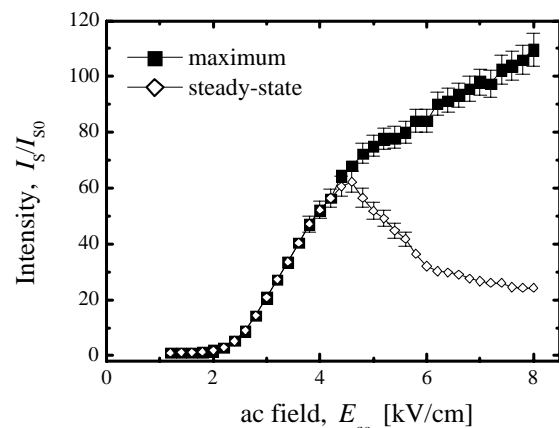


Fig. 3. The signal gain in the steady state and in maximum as a function of the applied field.

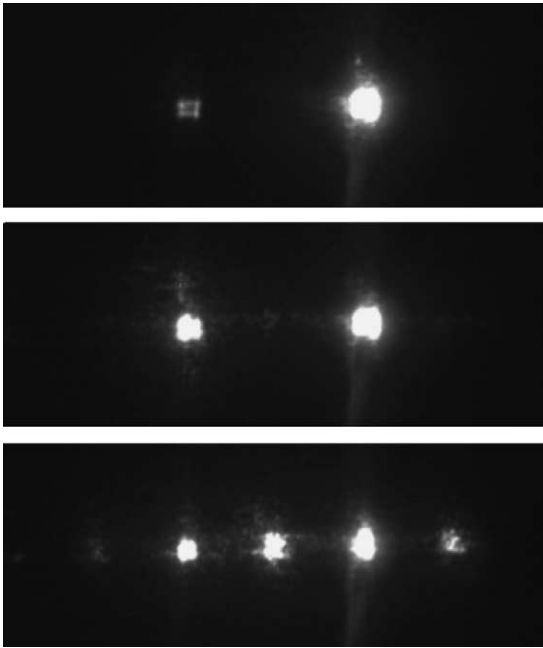


Fig. 4. Intensity patterns taken from screen behind the sample at different external field E ; upper picture: $E = 0$, middle picture: $E = 4.2$ kV/cm; bottom picture: $E = 8$ kV/cm.

when 8 kV/cm is applied to the crystal. Apart from two transmitted beams, an additional beam is observed which propagate exactly in-between recording beams. This beam corresponds to diffraction from grating with grating vector fractional to the principal grating vector \mathbf{K} , i.e. $\mathbf{K}/2$. That is why such phenomenon is called generation of spatial subharmonics. In our case higher orders of diffraction are also visible in addition to zero order of $\mathbf{K}/2$ subharmonic beam.

First spatial subharmonics were observed in $\text{Bi}_{12}\text{SiO}_{20}$ crystal [10], then their generation was achieved in all sillenites and recently in CdTe [11]. The origin of spatial subharmonics is related to excitation of space-charge waves (SCW) [12]. The SCW are the waves of traps recharging which can be excited in a material with large mobility-lifetime product in the presence of electric field [13]. The spatial frequency of the SCW is determined by crystal parameters and field amplitude [12]. The larger is field the smaller is spatial frequency of the SCW (larger is wavelength of the SCW) and the stronger are SCW. If spatial frequency of the grating is close to the spatial frequency of the SCW the resonant excitation of the SCW takes place and grating is increased considerably. Subharmonics generation occurs when the spatial frequency of the grating is integer fractional of the SCW spatial frequency.

Generation of $\mathbf{K}/2$ subharmonics occurs in our sample when field exceeds 4.4 kV/cm. The SCW becomes stronger with field growth and intensity of the subharmonic beam increases. We measure temporal dynamics of the amplified signal and subharmonic beam, which are shown in Fig. 5. Data of this figure demonstrate that intensity of the signal beam decreases when subharmonic beam is developing. Such re-

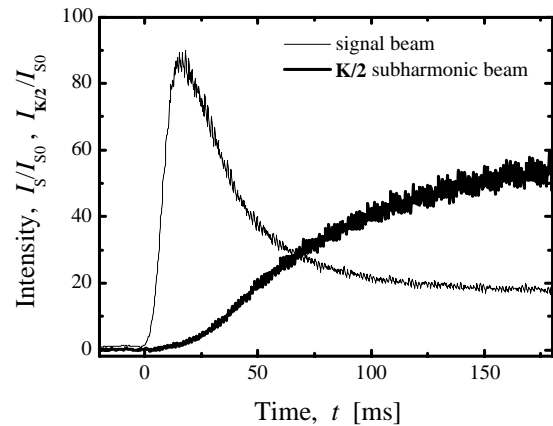


Fig. 5. Temporal dynamics of the amplified signal and subharmonic beam measured at $E = 7$ kV/cm.

duction of two-wave mixing gain was reported for $\text{Bi}_{12}\text{SiO}_{20}$ [14] previously. The origin of the phenomenon is obvious. It is related to competition between signal and subharmonic beam. When part of the pump light is diffracted from the subharmonic grating signal amplification decreases.

Thus, the field, which effectively increases signal gain, is limited by the threshold field of the subharmonics generation. The steady state two-beam coupling amplification even decreases at larger field. However, spatial frequency of the grating can be optimized to match the SCW spatial frequency at higher field. In our sample the wavelength of the SCW is about $85 \mu\text{m}$ at $E = 8$ kV/cm. To agree the recording grating with the SCW at this field the grating spacing is changed to $\Lambda \approx 85 \mu\text{m}$ (free space angle between recording beams $2\theta \approx 0.7^\circ$). There is no transient peak in signal amplification dynamics and 120-times steady state gain is measured at this grating spacing with $E = 8$ kV/cm. For our 1-cm thick sample this value corresponds to exponential gain factor $\Gamma \approx 4.8 \text{ cm}^{-1}$. This gain factor is eight-times larger than the absorption constant of the crystal $\alpha \approx 0.6 \text{ cm}^{-1}$, so amplification considerably overcoming losses is achieved.

In conclusion, we have demonstrated that two-beam coupling gain in ac-biased CdTe:Ge depends strongly on phenomena related to the SCW excitation. In wide range of grating spacings the field at which amplification of the signal beam is the largest is limited by threshold field of the spatial subharmonics generation. To achieve large gain spatial frequency of the recording grating should correspond to eigen spatial frequency of the SCW at given field. Up to 120-times steady state signal gain is reached in studied CdTe sample with such correspondence.

Acknowledgements

Authors are grateful to S. Odoulov for helpful discussions. Financial support of Civilian Research and Development Foundation under Award #UP2-536 is gratefully acknowledged.

References

- [1] K. Tada, M. Aoki, *Jpn. J. Appl. Phys.* 10 (1971) 998.
- [2] R.B. Bylisma, P.M. Bridenbaugh, D.H. Olson, A.M. Glass, *Appl. Phys. Lett.* 51 (1987) 889.
- [3] R.N. Schwartz, C.-C. Wang, S. Trivedi, G.V. Jagannathan, F.M. Davidson, Ph.R. Boyd, U. Lee, *Phys. Rev. B* 55 (1997) 15378.
- [4] S. Odoulov, S. Slussarenko, K. Shcherbin, *Sov. Techn. Phys. Lett.* 15 (1989) 417.
- [5] K. Shcherbin, V. Volkov, V. Rudenko, S. Odoulov, A. Borshch, Z. Zakharuk, I. Rarenko, *Phys. Stat. Sol. (a)* 183 (2001) 337.
- [6] K. Shcherbin, F. Ramaz, B. Farid, B. Briat, H.-J. von Bardeleben, in: P.E. Andersen et al. (Eds.), *Trends in Optics and Photonics*, vol. 27, OSA, Washington, DC, 1999, pp. 54–58.
- [7] J.P. Huignard, A. Marrakchi, *Opt. Commun.* 249 (1981) 38.
- [8] S.I. Stepanov, M.P. Petrov, *Opt. Commun.* 292 (1985) 53.
- [9] M. Ziari, W.H. Steier, P.M. Ranon, M.B. Klein, S. Trivedi, *J. Opt. Soc. Am. B* 9 (1992) 1461.
- [10] S. Mallick, B. Imbert, H. Ducollet, J.-P. Herriau, J.-P. Huignard, *J. Appl. Phys.* 63 (1988) 5660.
- [11] K. Shcherbin, *Appl. Phys. B* 71 (2000) 123.
- [12] B. Sturman, A. Bledowski, J. Otten, K. Ringhofer, *J. Opt. Soc. Am. B* 10 (1993) 1919.
- [13] R.F. Kazarinov, R.A. Suris, B.I. Fuks, *Sov. Phys. Semicond.* 7 (1973) 480.
- [14] A. Grunnet-Jepsen, L. Solymar, C.H. Kwak, *Opt. Lett.* 19 (1994) 1299.